





## Research Article

# Inhibition of the filamentation of *Candida albicans* by *Borojoa patinoi* silver nanoparticles

Marcela Gómez-Garzón<sup>1</sup>  · Luz D. Gutiérrez-Castañeda<sup>2</sup> · Camilo Gil<sup>1</sup> · Carlos H. Escobar<sup>1</sup> · Ana P. Rozo<sup>3</sup> · María E. González<sup>3</sup> · Edgar V. Sierra<sup>3</sup>

Received: 1 October 2020 / Accepted: 28 December 2020 / Published online: 25 January 2021  
© The Author(s) 2021 

## Abstract

*Candida albicans* is fungus capable of changing from yeast to filamentous form when it's transformed from a normal commensal to an opportunistic pathogen. The development of alternatives that interfere with this transition could be an effective way to reduce candidiasis. In this regard, evaluate the inhibitory effect of two *Borojoa patinoi* silver nanoparticles (AgNPs) produced by green synthesis at 5 °C and 25 °C on the process of filamentation of *Candida albicans*. The percentage of inhibition of filamentous forms of *C. albicans* ATCC10231 and *C. albicans* SC5314 with AgNPs was determined. Results showed that temperature of synthesis affected both the shape and size of silver nanoparticles synthesized using *Borojoa patinoi* extracts. The inhibition percentage of filamentous forms of *Candida albicans* ATCC10231 when treated with silver nanoparticles synthesized at 5 °C was 85.9% and at 25 °C it was 40%. *C. albicans* SC5314 when treated with AgNP synthesized at 5 °C was 97.2% and at 25 °C it was 64%. Cell toxicity assay showed that at 100ng/ml, AgNPs synthesized at 25 °C were safe in MES-OV CRL-3272 cell line. Our results showed that the silver nanoparticles obtained from *Borojoa patinoi* are inhibitors of the filamentous process of *C. albicans*.

**Keywords** Filamentation · *Candida albicans* · Silver nanoparticles · *Borojoa patinoi*

## 1 Introduction

*Candida albicans* is a polymorphic fungus, capable of developing reversible morphological changes, between yeast and filamentous form. This form is acquired when it's transformed from a normal commensal to an opportunistic pathogen. The development of alternatives that interfere with this transition could be an effective way to reduce candidiasis, including those related with the super infection of medical devices Arkowitz and Bassilana [2].

There are several reports of the antiseptic capability of metal nanoparticles, including those made with silver [39]; Gordienko, Palchikova et al. [8]. However, the nanoparticle

synthesis must be optimized to make them secure for humans Mathur, Jha et al. [20]; Souza, da Silva et al. [32].

The *bottom up* procedure for nanoparticles synthesis, consist of forming metal agglomerates by chemical reducing metal inorganic ions (gold, silver, iron and metal oxides). Recently have it been proposed that these nanoparticles could be produced harnessing the reducing capacities of metabolites and proteins in biological systems, known as green synthesis. The green synthesis of silver nanoparticles using different biological systems (including viruses, bacteria, fungus and plants), has the advantages of being a simple, safe and low cost Nasrollahzadeh, Mahmoudi-Gom Yek et al. [22]. The nanoparticles produced through the green synthesis have been

✉ Marcela Gómez-Garzón, mgomez@fucsalud.edu.co | <sup>1</sup>Ciencias Básicas, Fundación Universitaria de Ciencias de la Salud, Bogotá, Colombia. <sup>2</sup>Grupo Ciencias Básicas en Salud, Instituto de Investigación, Fundación Universitaria de Ciencias de la Salud, Bogotá, Colombia. <sup>3</sup>Facultad de Ingeniería y Ciencias Básicas, Universidad Central, Bogotá, Colombia.



proved to have fungicidal action and control of biofilm formation by *Candida albicans* Khatoon, Sharma et al. [13].

Plants, such as *Borojoa patinoi* (borojo), are able to reduce inorganic ions in metallic nanoparticles both in intra and extracellular compartments Rajeshkumar and Bharath [28]. Moreover the plant extracts have a broad spectrum of chemical components that facilitate the bioreduction and stabilization of nanoparticles, conferring it antibactericidal capabilities (Escarcega-Gonzalez, Garza-Cervantes et al. [5]; Nasrollahzadeh, Mahmoudi-Gom Yek et al. [22]; Ali, Ikram et al. [1]).

The *Borojoa patinoi* is a fruit native to Colombia, it belongs to the Rubiaceae family and is known for its energy and nutritional capacity. The fruit has high concentrations of amino acids and phosphorus essential for humans. It is used in traditional and popular medicine as a diuretic, healing, aphrodisiac, antimicrobial and antitumor Giraldo, Rengifo et al. [7]; Sotelo D, Casas F et al. [31]

The purpose of this work was to evaluate the inhibitory effect of silver nanoparticles of *Borojoa patinoi* produced at 5 °C and 25°C on the process of filamentation of *Candida albicans*. We hypothesized that the synthesis temperature of nanoparticles affects their characteristics and antimicrobial effects.

## 2 Experimental details

### 2.1 Materials

Commercial extract of *Borojoa patinoi* was provided by Phitother Laboratories. Silver nitrate (AgNO<sub>3</sub>) was acquired from Panreac (> 99%) and the distilled / deionized water was obtained from an EasyPure Rodi Ultrapure water purification system with a resistivity higher than 18.2 MΩ.cm. The solvents used in the rinsing of the nanoparticles and the preparation of the microscopy samples were 96% ethanol, in addition to the 1-propanol Reagent ACS ≥99.5% were procured from Sigma Aldrich. For the microbiological tests, Sabouraud Dextroxa Oxoid Agar, YPD medium and Trypticase soy broth (Merck), Rabbit Plasma with EDTA (BBL Microbiology Systems) and Calcofluor white dye (Sigma Aldrich) were used. Cytotoxicity was evaluated by using Mc Coy 5A culture medium (Sigma- Aldrich ®) fetal bovine serum (FBS), 3- (4,5-dimetiltiazol-2-il) –2,5-difeniltetrazolio bromuro (MTT) by Trevigen® and dimethylsulfoxide (DMSO)

### 2.2 Preparation and characterization of silver nanoparticles

AgNPs were obtained by green synthesis from *Borojoa patinoi* extract. Briefly, they were prepared by mixing 10

mM AgNO<sub>3</sub> in *Borojoa patinoi* extract at 2% w / v. A reaction product was carried out at 5°C (AgNPs-43) or at 25°C (AgNPs-31), in darkness until day 58.

The reduction of silver ions was confirmed by the color change from yellow to red-brown. The UV-vis spectra of the reaction mixture were periodically measured in a Thermo Scientific Genesys 10 UV-Vis Spectrometer between 200 and 1100 nm, operated at a resolution of 3 nm.

The washes were performed by centrifugation for 30 minutes at 10,000 rpm to purify the AgNPs. The sediment was dispersed in deionized water to remove the water-soluble biomolecules. The samples were dried in an oven at 60 °C for 24h.

The hydrodynamic size of the particles and the polydispersity index (PDI) of the silver nanoparticles were analyzed by means Dynamic Light Scattering (DLS) (Malvern Zetasizer Nano ZS90 Dynamic Light Scattering). The analysis of the samples was carried out in aqueous solution at a controlled temperature. The product of the synthesis was quantified by determining the weight of the sample on a dry petri dish: a previously homogenized 2 ml aliquot was taken, once these solutions were dried and cooled the AgNP's mass was calculated. The shape of the nanoparticles was determined by Transmission Electron Microscopy (TEM) and size measurements of the images were obtained using the ImageJ / Fiji 1 image processor.

## 3 Strains of *Candida albicans*

Two reference strains of *Candida albicans* from American Type Culture Collection (ATCC), *C. albicans* ATCC10231 and *C. albicans* SC5314 / ATCCMYA-2876 were tested. The strains were cultivated in Sabouraud Dextroxa Agar overnight at 37 °C. *Candida* cells were grown overnight in YPD medium (1% yeast extract, 2% peptone and 2% dextrose), the yeast concentration was adjusted spectrophotometrically to absorbance of 0.12 corresponding to 1×10<sup>6</sup> yeast/ml.

The effect of nanoparticles on the transition to filamentous form, the inhibitory effect of AgNPs-31 and AgNPs-43, was tested with the two strains of *C. albicans* as follows: 50μL of 1×10<sup>6</sup> yeast/ml, 75μL Trypticase-Soy broth, 50μL of Rabbit Plasma with EDTA, 25μL of AgNPs at 100μg / ml, and 10μL of Calcofluor white were mixed and incubated at 37 °C for 4 h. Each nanoparticle was evaluated in duplicates. For the positive control of filamentation, 50μL of 1×10<sup>6</sup> yeast/ml, 75μL Trypticase-Soy broth, 50μL of Rabbit Plasma with EDTA and 10μL of Calcofluor white were used. Quantification of inhibition of the budded-to-hyphal-form transition was accomplished by counting the number of individual budded cells versus the number of filamentous

form in the population. More than 100 cells were counted for each well in duplicate, and all assays were repeated at least twice Toenjes, Munsee et al. [35]; Romo, Pierce et al. [29]. Additionally, images of the cell morphology were obtained under a Leica DM 2500 microscope under fluorescence with the UV filter A (Exc: 340-380 / EspDic: 400 / Bar: 430), where the yeasts were observed stained silver blue.

## 4 Cell culture

The MES-OV CRL-3272™ cell line was obtained from ATCC® (American Type Culture Collection). The cell line were cultured in Corning Glass Culture Flasks from Sigma-Aldrich® and cultured in McCoy 5A medium supplemented with 10% SFB (v/v), and cultures were maintained at 37 °C, in a humid atmosphere containing 5% CO<sub>2</sub>.

## 5 Cell viability

The cytotoxic induced by nanoparticles was evaluated through the mitochondrial activity of cells incubated with AgNPs using the MTT assay. Fifty ng/mL or 100 ng/mL of nanoparticle were dissolved in Mc Coy 5A medium and sonicated by 10 min using ultrasonicator Elmasonic S30. Then,  $5 \times 10^5$  MES-OV cells were incubated with 50 ng/mL or 100 ng/mL the AgNPs for 24, 48 and 72h at 37 °C, in a humidified 5% CO<sub>2</sub>. The results were compared with effect of commercial nanoparticles (AgNPs, Sigma-Aldrich reference 730793, size of 20nm). MTT assay was realized after indicated times. Each cell group adding tetrazolium

salt (MTT reagent) and dark-incubated at 37 °C for 4 h. Formazan crystals generated by metabolically active cells were solubilized with detergent reagent and incubated for 4 h at 37 °C. Absorbance was read in a microplate reader at 650nm (Ultramark microplate reader. Model 8422, Bio-Rad). Cells without nanoparticles were used as control. Data were expressed as the percent SD of metabolic activity with respect to the non-inoculated controls using the following formula: (OD well of cells incubated with AgNPs (-blank))/ (mean OD non-inoculated cells well (-blank))  $\times 100$ .

## 6 Statistic evaluation

Experiments of filamentation were performed in duplicate. Experiments of cytotoxicity were performed by triplicate. The results were reported as mean and standard deviation. The statistical analysis was performed by descriptive statistics using frequencies and percentages using STATA (Version 15.0. Texas, StataCorp LLC)

## 7 Results and discussion

AgNPs were obtained through the reduction of silver ions added to the extract of the plant. Color change from yellow to red-brown indicated the formation of AgNPs. The formation and stability of the nanoparticles were evaluated by UV-Vis spectrophotometric analysis. The reaction progression upon formation of the AgNPs-31, synthesized at 25 °C, and AgNPs-43, synthesized at 5 °C, is shown in Fig. 1, with a peak occurring between 400 and 500 nm.

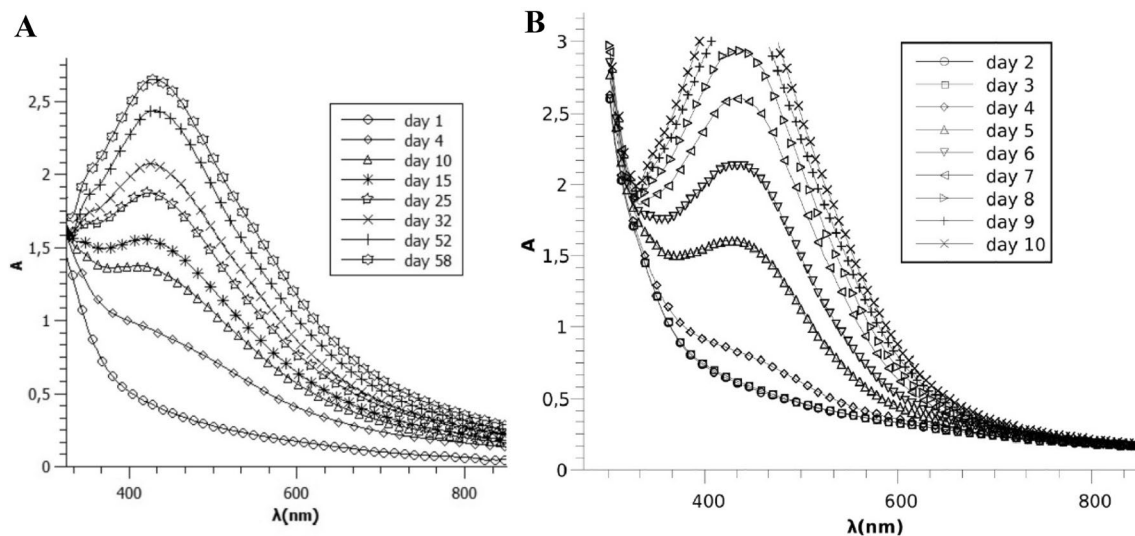


**Fig. 1** The reaction progression upon formation: **a** AgNPs-31 synthesized at 25 °C and **b** AgNPs-43, synthesized at 5 °C

The formation of nanoparticles due to the reduction of AgNO<sub>3</sub> during incubation with *Borojoa patinoi* extract is evident by the change in the color of the reaction mixture, which turned from yellow to red-brown. During the process of green synthesis, the brown color is due to the excitation in the absorption spectrum of the plasmon vibrations of the surface of the plant extracts at different wavelengths, ranging from 300 to 700 nm generally with a peak at 435 Ghareib, Tahon et al. [6]. The surface plasmon resonance band is influenced by the size, shape, morphology, composition and dielectric environment in the synthesized nanoparticles Chahardoli, Karimi et al. [4].

In the DLS size distribution of the AgNPs-31, a peak of 213.2 d.nm with an intensity of 95.9% was observed, a second peak of 4544 d.nm with an intensity of 2.6% and a third peak of 10.5 d.nm with intensity of 1.5%. For the AgNPs-43 the first peak of 238.7 d.nm with intensity of 92.9%, a second peak of 22.64 d.nm with intensity of 5.2% and a third peak of 4734 d.nm and intensity of 1.8% (Fig. 2). The differences in the average hydrodynamic diameter and in the polydispersity index (PDI) were established according to the temperature change (Fig. 3). The final concentration of the nanoparticles obtained by green synthesis was 275 µg/ml for AgNPs-31 and 150 µg/ml for AgNPs-43.

The AgNPs rate formation was related to the reaction temperature such that an increase in the temperature allowed the production of particles at a faster rate. The peak absorption of 435nm indicating the formation of AgNPs, confirmed by the slight change in the maximum of the absorption spectra indicating that the silver had been completely reduced, was reached in 8 days at 5 °C but took 52 days at 25 °C; additionally a higher concentration was obtained at 25 °C (275 µg/ml).

The trimodal distribution of the AgNPs were obtained by DLS. The area under the curve indicated that the highest proportion of particles were of large diameters: 213.2 nm for AgNPs-31 and 238.7 nm for AgNPs-43. Only 1.5%

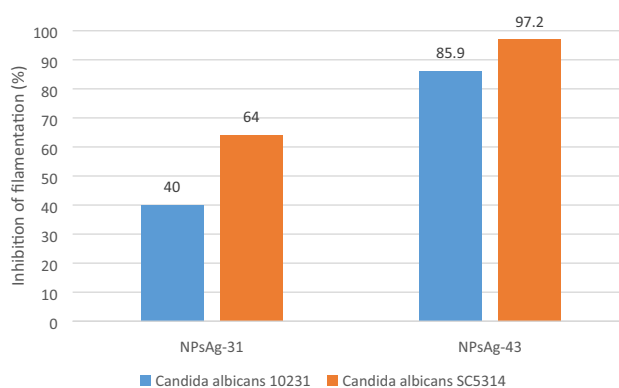


**Fig. 3** The differences in the average hydrodynamic diameter (d.nm) and in the polydispersity index (PDI) according to the temperature change

of the AgNPs-31 corresponded to particles of small size (10.5nm), while the rest corresponded to the large size (213.2nm), while the rest corresponded to the large size. According to the polydispersity index (PDI) of all the experiments (greater than 0.1) we found that polydispersed solutions were synthesized.

The morphology, size and shape were determined by TEM. AgNPs-31 were spherical shapes of 18–45nm and rods of 31–38nm in width by 50–75nm length. AgNPs-43 were only spherical shapes of 20.6–330nm (Fig. 4).

The characterization of the samples by TEM demonstrated the presence for AgNPs-31 of spherical shapes of 18–45nm and rods with 31–38 in width by 50–75 in length for AgNPs-31 and only spherical shapes of 20.6–330nm for AgNPs-43. Similar geometries were previously reported in other silver nanoparticles synthesized by green synthesis Ma, Su et al. [19]; Taha, Hawar et al. [33].

The nanoparticles show mechanisms of fungicidal action different from traditional antifungals, thus providing an alternative to the growing resistance Chahardoli, Karimi et al. [4]. The NPs can cross the cell membrane and reach the intracellular space, where they generate a large

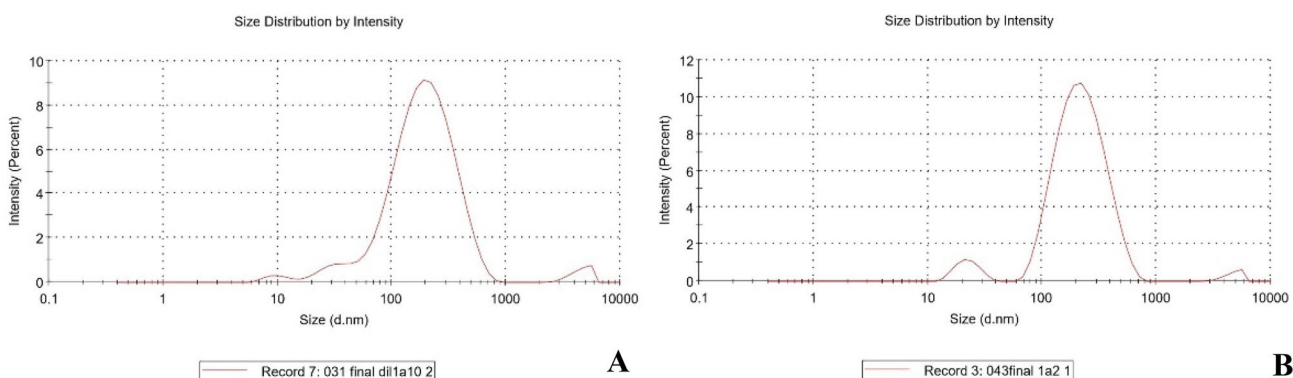


**Fig. 2** Dynamic Light Scattering (DLS) size distribution of the **a** AgNPs-31 and **b** AgNPs-43

**Fig. 4** Representative Transmission Electron Microscopy (TEM) micrographs for the **a** AgNPs-31 and **b** AgNPs-43

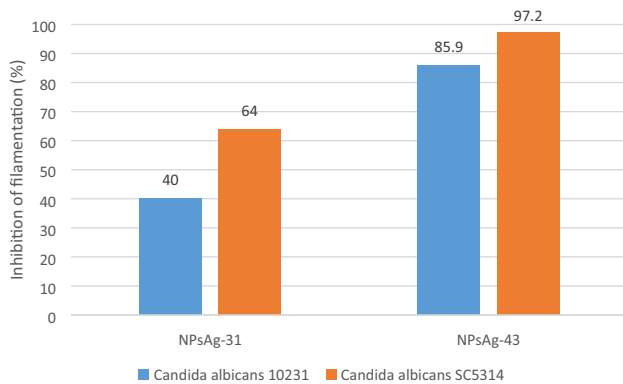
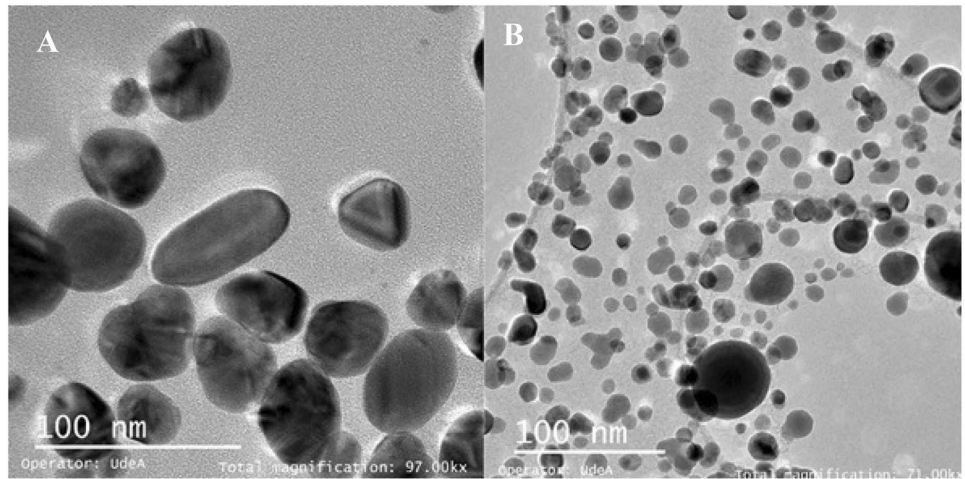


**Fig. 5** Inhibition of filamentation of AgNPs-31 and AgNPs-43 on *C. albicans* ATCC 10231 and *C. albicans* SC 5314

oxidative imbalance by raising the levels of reactive oxygen species (ROS). Large ROS imbalance can degrade the essential components of the cells responsible for maintaining the physiological and morphological functions of the cells. ROS cause damage at the membrane and DNA level, leading to the death of the fungus Wang, Hu et al. [38]; Uddin, Siddique et al. [36].

The effect of AgNPs-31 and AgNPs-43 on *C. albicans* ATCC10231 and *C. albicans* SC5314 was determined by the percentage of inhibition of filamentation. The result revealed that *C. albicans* SC5314 presented 64% with AgNPs-31 and 97.2% with AgNPs-43 (average 80.6%), while *C. albicans* ATCC10231 40% with AgNPs-31 and 85.9% with AgNPs-43 (average 63.0%) (Fig. 5). The filamentation

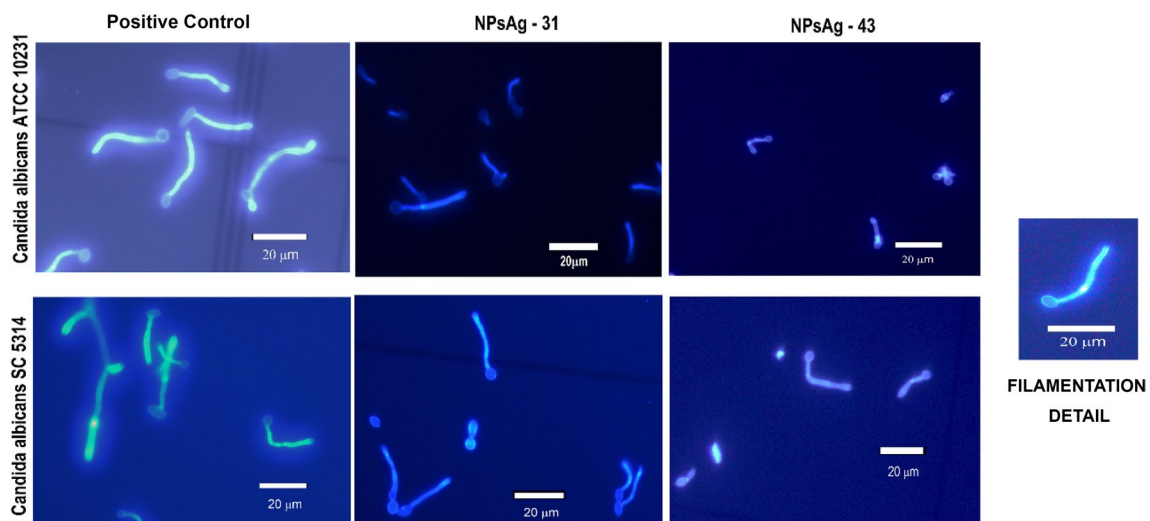


**Fig. 6** The filamentation morphology of positive controls, NPsAg-31 and NPsAg-43 of both *Candida albicans* SC 5314 and ATCC 10231, using fluorescence with Calcofluor white

morphology was documented under fluorescence with Calcofluor white (Fig. 6).

The two clinical isolates SC5314 and ATCC10231 of *C. albicans* both differ in their ability to invade host tissue and cause experimental infections. Strain SC5314 was isolated in 1984 from a candidemia patient and is considered a reference of the invasive strain (Odds, Brown et al. [24]. Meanwhile the strain ATCC10231 is strongly attenuated in virulence due to gene duplication or loss of an allele (hewes, Moran et al. [34]. When comparing the two species of *Candida albicans*, we observed that *C. albicans* SC5314 was more sensitive to both AgNPs than *C. albicans* ATCC10231, resulting in a higher percentage of inhibition of filamentous forms necessary to initiate an invasive process (80.6% vs 63.0% respectively). Strain ATCC10231 is frequently used for pharmacological purposes, although several studies have shown that this strain produces shorter germ tubes compared to strain SC5314 Thewes, Moran et al. [34]; Romo, Pierce et al. [29]; Bartelli, Bruno et al. [3]. Our results suggest that NPsAg interfered with the cAMP-PKA and MAPK pathways, which are widely employed by fungal pathogens to control the morphological transition Meng, Zhao et al. [21].

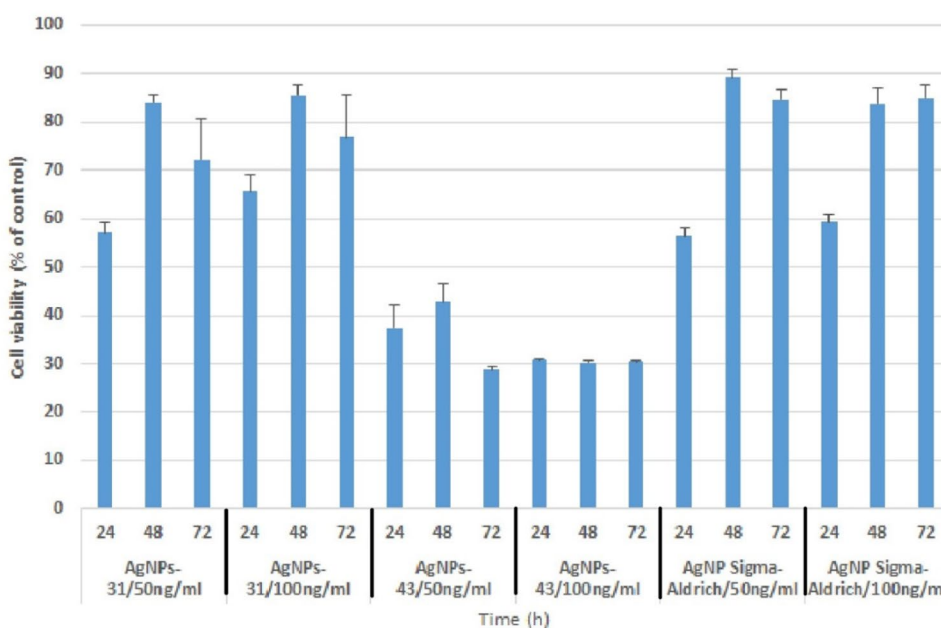
The microscopic evaluation of the yeasts with Calcofluor White, allowed us to observe the inhibitory effect of the AgNPs. Scarce filamentation and predominance of blastoconidia was seen in Fig. 6. The effectiveness of AgNPs against *C. albicans* has been shown to be due to morphological changes in fungal cells, damage to the membrane, formation of pores that cause the release of ions and induced alterations in multiple cellular targets Wady, Machado et al. [37]; Radhakrishnan, Reddy Mudiam

et al. [26]. In a study with SEM, it was observed that the structure of *C. albicans* was lost when treated with AgNPs, due to the rupture of the membrane and cell wall; additionally, this study showed inhibition of filamentation. Using TEM it was shown that there was a change in the permeabilization of the cell wall and subsequent explosion of the inner layers of the fungal wall Lara, Romero-Urbina et al. [17].

Several studies have shown that AgNPs synthesized by physical or chemical routes have the potential to induce toxicity to cells of animals. Nanoparticles absorbed to an external surface of organisms, however, can in some cases damage cell walls or cell membranes or cause a steady release of ions that affect the cell Liu, Wu et al. [18]; Newton, Puppala et al. [23]; Seitz, Rosenfeldt et al. [30]; Hu, Chen et al. [10]. The average viability of cells treated with AgNPs-31 in 50 ng/mL and 100 ng/mL concentrations varied between 57 and 86% at 24, 48 and 72h. This viability was similar to observed with the AgNPs Sigma-Aldrich®. The AgNPs-43 in 50 ng/mL and 100 ng/mL concentrations generated viability between 29 and 43% (Fig. 7). These results show that the sizes of the nanoparticles are determinants of the degree of cytotoxicity. How it was observed the larger particles (AgNPs-43) induced a greater cytotoxic effect, decreasing viability by more than 50% on average independent of incubation time and concentration. Likewise, the results shown here indicate that AgNP-31 are less toxic at concentrations of 50 ng/mL up to 100 ng/mL. This effect in the cell viability may be particularly important for clinical application.

The average toxicity against the cell line MES-OV CRL-3272 of AgNPs-31 at concentrations of 50 ng/ml

**Fig. 7** Cells viability of treatments with different concentrations of Ag-NPs-31 and AgNPs-43 after 12, 24 and 48hs



and 100 ng/ml was 28.5%, while AgNPs-43 was 64% (s 7). Small nanoparticles (10–50nm) enter cells more easily than larger ones (250nm) (Hsin, Chen et al. 2008). The high toxicity is due to the ease causing damage to the membrane, altering the lysosomal activity and increases the production of intracellular reactive oxygen species (ROS), leading to mitochondria-dependent apoptosis Liu, Wu et al. [18]. Only 1.5% of the AgNPs-31 corresponded to particles of small size (10.5nm), while 5.2% of the AgNPs-41 22.64nm, this would explain its greater toxicity.

Different factors such as light, pH, temperature and concentration of metal ions play an important role in the synthesis of nanoparticles Rai and Yadav [27]. According to the percentages of filament inhibition, it is clear that the synthesis temperature of the AgNPs significantly affects their antifungal activity. At high temperature, the kinetic energy of the molecules increases, and the silver ions are consumed faster, leaving less possibilities of growth in the size of the particles. Therefore, smaller particles of almost uniform size distribution are formed at higher temperatures Jain and Mehata [12]. Figure 3 shows the size of the AgNPs and the polydispersity, demonstrating that the increase of 20 °C in the temperature led to the formation of AgNPs that were 14.3nm smaller and a 0.017 decrease in the polydispersity index, indicating that in both temperatures the particles were homogeneous.

The shape and size of AgNPs are directly related to the cell internalization process, which is based on endocytosis. The size range of nanoparticles small enough to pass through the bilayer of phospholipids, is from 10 to 500 nm, our AgNPs are in this range (Kou, Sun et al. 2013; Kou, Bhutia et al. 2018).  $\Omega$  is defined as the angle between the normal membrane of the cell at the junction point and the line that defines the curvature of the nanoparticle at the point of endocytosis. The particles are internalized successfully at  $\Omega \leq 45^\circ$  and the internalization of the particles can be inhibited if  $\Omega > 45^\circ$ . Studies on bacteria, yeasts, algae, crustaceans and mammalian cells have shown that the toxicity of nanoparticles depends on their shape Pal, Tak et al. [25]; Ivask, Kurvet et al. [11]; Kim, Park et al. [14]. Nanoparticles with the same surface area but with different shapes present different areas in terms of active facets. The spherical forms of AgNPs-43 were very efficient in entering yeast and therefore inhibiting filamentation. On the other hand, rod shapes of AgNPs-31 could not be transported through the membrane, this explains the higher percentages of inhibition of AgNPs synthesized at 5°C. The hypothesis was accepted since we observed that the AgNPs inhibit the filamentous forms and this capacity was dependent on the synthesis temperature in AgNPs.

## 8 Conclusions

The reaction temperature plays a key role in the shape and size of the nanoparticles obtained by green synthesis. *Borojoa patinoi* extract successfully produced two different nanoparticles, AgNPs-31, synthesized at 25 °C, with spherical shapes of 18–45nm and rods 31–38 wide by 50–75 in length, and AgNPs-43, synthesized at 5 °C, only with spherical shapes of 20.6–330nm. The AgNPs-43 showed a greater inhibitory effect on the filamentation process of the two species of *Candida albicans* evaluated and significant toxicity against the cell line MES-OV CRL-3272 at 50 and 100 ng/ml.

**Acknowledgements** The authors thank Adriana Morales for critical revision of the manuscript, and we would like to express our gratitude to Phitother Laboratories for providing the *Borojoa* extract.

## Compliance with ethical standards

**Conflict of interest** The authors declare that they have no conflict of interest

**Open Access** This article is licensed under a Creative Commons Attribution 4.0 International License, which permits use, sharing, adaptation, distribution and reproduction in any medium or format, as long as you give appropriate credit to the original author(s) and the source, provide a link to the Creative Commons licence, and indicate if changes were made. The images or other third party material in this article are included in the article's Creative Commons licence, unless indicated otherwise in a credit line to the material. If material is not included in the article's Creative Commons licence and your intended use is not permitted by statutory regulation or exceeds the permitted use, you will need to obtain permission directly from the copyright holder. To view a copy of this licence, visit <http://creativecommons.org/licenses/by/4.0/>.

## References

1. Ali M, Ikram M et al (2020) "Green synthesis and evaluation of n-type ZnO nanoparticles doped with plant extract for use as alternative antibacterials. *Appl Nanosci* 10(10):3787–3803
2. Arkowitz RA, Bassilana M (2019) Recent advances in understanding *Candida albicans* hyphal growth. *F1000Res*. <https://doi.org/10.12688/f1000research.18546.1>
3. Bartelli TF, Bruno D et al (2018) "Whole-genome sequences and annotation of the opportunistic pathogen *Candida albicans* strain SC5314 grown under two different environmental conditions. *Genom Announc*. <https://doi.org/10.1128/genomEA.01475-17>
4. Chahardoli A, Karimi N et al (2017) Biosynthesis, characterization, antimicrobial and cytotoxic effects of silver nanoparticles using *Nigella arvensis* seed extract. *Iran J Pharm Res* 16(3):1167–1175
5. Escarcega-Gonzalez CE, Garza-Cervantes JA et al (2018) In vivo antimicrobial activity of silver nanoparticles produced via a green chemistry synthesis using *Acacia rigidula* as a reducing and capping agent. *Int J Nanomed* 13:2349–2363

6. Ghareib M, Tahon MA et al (2016) Rapid extracellular biosynthesis of silver nanoparticles by *Cunninghamella phaeospora* culture supernatant. *Iran J Pharm Res* 15(4):915–924
7. Giraldo CI, Rengifo L et al (2004) Determinación del sexo en borojó (*Borojoa patinoi*, Cuatrecasas) mediante marcadores moleculares. *Revista Colombiana de Biotecnología* 6(2):2004
8. Gordienko MG, Palchikova VV et al (2019) Antimicrobial activity of silver salt and silver nanoparticles in different forms against microorganisms of different taxonomic groups. *J Hazard Mater* 378:120754
9. Hsin YH, Chen CF et al (2008) The apoptotic effect of nanosilver is mediated by a ROS- and JNK-dependent mechanism involving the mitochondrial pathway in NIH3T3 cells. *Toxicol Lett* 179(3):130–139
10. Hu Y, Chen X et al (2018) Distinct toxicity of silver nanoparticles and silver nitrate to *Daphnia magna* in M4 medium and surface water. *Sci Total Environ* 618:838–846
11. Ivask A, Kurvet I et al (2014) Size-dependent toxicity of silver nanoparticles to bacteria, yeast, algae, crustaceans and mammalian cells in vitro. *PLoS One* 9(7):e102108
12. Jain S, Mehata MS (2017) Medicinal plant leaf extract and pure flavonoid mediated green synthesis of silver nanoparticles and their enhanced antibacterial property. *Sci Rep* 7(1):15867
13. Khatoun N, Sharma Y et al (2019) Mode of action and anti-*Candida* activity of *Artemisia annua* mediated-synthesized silver nanoparticles. *J Mycol Med* 29(3):201–209
14. Kim DH, Park JC et al (2017) Effect of the size and shape of silver nanoparticles on bacterial growth and metabolism by monitoring optical density and fluorescence intensity. *Biotechnol Bioprocess Eng* 22(2):210–217
15. Kou L, Bhutia YD et al (2018) Transporter-guided delivery of nanoparticles to improve drug permeation across cellular barriers and drug exposure to selective cell types. *Front Pharm* 9:27–27
16. Kou L, Sun J et al (2013) The endocytosis and intracellular fate of nanomedicines: implication for rational design. *Asian J Pharm Sci* 8(1):1–10
17. Lara HH, Romero-Urbina DG et al (2015) Effect of silver nanoparticles on *Candida albicans* biofilms: an ultrastructural study. *J Nanobiotechnol* 13:91
18. Liu W, Wu Y et al (2010) Impact of silver nanoparticles on human cells: effect of particle size. *Nanotoxicology* 4(3):319–330
19. Ma L, Su W et al (2017) Optimization for extracellular biosynthesis of silver nanoparticles by *Penicillium aculeatum* Su1 and their antimicrobial activity and cytotoxic effect compared with silver ions. *Mater Sci Eng C Mater Biol Appl* 77:963–971
20. Mathur P, Jha S et al (2018) Pharmaceutical aspects of silver nanoparticles. *Artif Cells Nanomed Biotechnol* 46(sup1):115–126
21. Meng L, Zhao H et al (2019) Inhibition of Yeast-to-hypha transition and virulence of *Candida albicans* by 2-Alkylaminoquinoline Derivatives. *Antimicrob Agents Chemother* 63(4):e01891–01818
22. Nasrollahzadeh M, Mahmoudi-Gom Yek S et al (2019) Recent developments in the plant-mediated green synthesis of Ag-based nanoparticles for environmental and catalytic applications. *Chem Rec* 19(12):2436–2479
23. Newton KM, Puppala HL et al (2013) Silver nanoparticle toxicity to *Daphnia magna* is a function of dissolved silver concentration. *Environ Toxicol Chem* 32(10):2356–2364
24. Odds FC, Brown AJ et al (2004) *Candida albicans* genome sequence: a platform for genomics in the absence of genetics. *Genom Biol* 5(7):230
25. Pal S, Tak YK et al (2007) Does the antibacterial activity of silver nanoparticles depend on the shape of the nanoparticle? A study of the Gram-negative bacterium *Escherichia coli*. *Appl Environ Microbiol* 73(6):1712–1720
26. Radhakrishnan VS, Reddy Mudiam MK et al (2018) Silver nanoparticles induced alterations in multiple cellular targets, which are critical for drug susceptibilities and pathogenicity in fungal pathogen (*Candida albicans*). *Int J Nanomed* 13:2647–2663
27. Rai M, Yadav A (2013) Plants as potential synthesiser of precious metal nanoparticles: progress and prospects. *IET Nanobiotechnol* 7(3):117–124
28. Rajeshkumar S, Bharath LV (2017) Mechanism of plant-mediated synthesis of silver nanoparticles - A review on biomolecules involved, characterisation and antibacterial activity. *Chem Biol Interact* 273:219–227
29. Romo JA, Pierce CG et al (2017) Development of Anti-virulence approaches for candidiasis via a novel series of small-molecule inhibitors of *Candida albicans* filamentation. *mBio*. <https://doi.org/10.1128/mBio.01991-17>
30. Seitz F, Rosenfeldt RR et al (2015) Effects of silver nanoparticle properties, media pH and dissolved organic matter on toxicity to *Daphnia magna*. *Ecotoxicol Environ Saf* 111:263–270
31. Sotelo D, I., N. Casas F, et al (2010) Borojó (*Borojoa patinoi*): fuente de polifenoles con actividad antimicrobiana. *Vitae* 17:329–336
32. Souza LRR, da Silva VS et al (2018) Toxic and beneficial potential of silver nanoparticles: the two sides of the same coin. *Adv Exp Med Biol* 1048:251–262
33. Taha ZK, Hawar SN et al (2019) Extracellular biosynthesis of silver nanoparticles from *Penicillium italicum* and its antioxidant, antimicrobial and cytotoxicity activities. *Biotechnol Lett* 41(8–9):899–914
34. Thewes S, Moran GP et al (2008) Phenotypic screening, transcriptional profiling, and comparative genomic analysis of an invasive and non-invasive strain of *Candida albicans*. *BMC Microbiol* 8:187
35. Toenjes KA, Munsee SM et al (2005) Small-molecule inhibitors of the budded-to-hyphal-form transition in the pathogenic yeast *Candida albicans*. *Antimicrob Agents Chemother* 49(3):963–972
36. Uddin AKMR, Siddique MAB et al (2020) Cocos nucifera leaf extract mediated green synthesis of silver nanoparticles for enhanced antibacterial activity. *J Inorg Organomet Polym Mater*. <https://doi.org/10.1007/s10904-020-01506-9>
37. Wady A, Machado A et al (2012) Evaluation of *Candida albicans* adhesion and biofilm formation on a denture base acrylic resin containing silver nanoparticles. *J Appl Microbiol* 112:1163–1172
38. Wang L, Hu C et al (2017) The antimicrobial activity of nanoparticles: present situation and prospects for the future. *Int J Nanomed* 12:1227–1249
39. Wilkinson LJ, White RJ et al (2011) Silver and nanoparticles of silver in wound dressings: a review of efficacy and safety. *J Wound Care* 20(11):543–549

**Publisher's Note** Springer Nature remains neutral with regard to jurisdictional claims in published maps and institutional affiliations.